Desalination and Water Treatment
www.deswater.com

doi: 10.1080/19443994.2014.985720

57 (2016) 2877–2886
February

Taylor & Francis
Taylor & Francis Group

Several salts of pyrophosphoric heteropoly acid: characterization and ion-exchange behavior for calcium removal from manganiferous water

Huixin Zhang*, Tingru Yang, Qian Dou, Dongxue Sun, Dongdong Wang

School of Chemistry and Chemical Engineering, Hebei University of Technology, Tianjin 300130, China,
emails: zhanghuixin@hebut.edu.cn, zhang_huixin@aliyun.com (H. Zhang), yangtingru1989@163.com (T. Yang), douqian_586x@126.com (Q. Dou), xiaoxue_19870613@126.com (D. Sun), 1064511836@qq.com (D. Wang)

Received 5 January 2014; Accepted 24 October 2014

ABSTRACT

In this study, five salts of pyrophosphoric heteropoly acid were synthesized as ion exchanger to remove Ca^{2+} in manganiferous water and characterized by Fourier Transform Infrared spectroscopy and scanning electron microscope. Their performances like ion-exchange capacities, selectivities were tested and the results were compared with zirconium phosphate and molecular sieves (13X and 5A). It can be found that Ca exchange reaction is easy to occur on these ion exchangers. The outcomes for zirconium tungstophosphate (ZWPP) were the best among the mentioned salts, its dynamic exchange capacity has been verified through static and column experiments. The specific surface areas, pore structure, and particle size of ZWPP were also calculated, therein ZWPP being classified into materials with nanoparticles and mesoporosity. Therefore, the salts of pyrophosphoric heteropoly acids, especially ZWPP, can be used as a potential ion exchanger for Ca removal in processed water and effluents from metallurgical industries.

Keywords: Salts of pyrophosphoric heteropoly acid; Ca ion exchange; Manganiferous water

1. Introduction

Large quantities of discharged industrial wastes produced in the production of electrolytic metal manganese (EMM) have complicated components, and their direct emission forms serious environmental pollution. On the other hand, the tons of electrolytic manganese residue (EMR) produce a large sum of manganese slag percolate which not only pollute water resources and soil but also waste manganese resource, as it contains a great deal of manganese resources and small amounts of other elements such as calcium and magnesium. Due to growing awareness of the green economy and circular economy, efficient technologies have attracted lots of attention to effectively recycle manganese and revitalize wastewater with the expectation of economization of energy sources and thus reduction of emissions. However, the situation is often encountered that a tiny minority of impurities such as Ca^{2+} will be concentrated in the process of recycling manganese. Moreover, it is easy for Ca to form slightly soluble or insoluble salts especially in such effluents from EMM and EMR, bearing a great amount of SO_4^{2-}. Consequently, a greater impact will be brought about that a mass deposit and suspension will form and thus a sharp increase in turbidity will occur; this will give rise to serious disturbance to routine operation and

*Corresponding author.

practices both in wastewater treatment and manganiferous production. As a result, there is bound to be a quality deterioration in both recirculated manganese materials and final manganiferous products. Therefore, the removal of Ca^{2+} in lower content is of significance before waste treatment and reutilization.

Various conventional methods including biological [1], physical [2], or chemical processes [3] have been used to remove metal ions. However, these methods are not always efficient and they even have some disadvantages when it comes to low solute concentration [4]. Ion-exchange technology, due to its high removal rate, simple devices, and easy operation, has been much used with respect to the scholarly track and hold. But people have to attach great consideration to poor thermal stabilities, poor resistance to radiation, and high exchange potential for highly charged metal ions and unsatisfied recognition to the ions with the same valence during organic resins applications. By contrast, advancement in inorganic ion exchangers is not only due to their high stability, simple synthesis, and good compatibility to the environment, but also for their unusual selectivity for ionic species. Inorganic ion exchangers have been gaining popularity in wastewater treatment [5], especially for treatment of radioactive wastewater and organic wastewater [6–8] where high removal efficiency is required, even in water purification they have very good application prospect. Some encouraging results with ammonium molybdophosphatepolyacrylonitrile or transition metal hexacyanoferrate immobilized on diverse supports were reported as ion exchangers [9,10]. However, they have questionable thermal stability at elevated temperatures. Recently, some ion exchangers based on zirconium [11,12] were reported to remove radioactive cesium with high exchange capacity and considerable distribution coefficient, which is considered to play an increasing role in the selective removal of specific radio nuclides.

To remove Ca^{2+} in the manganese slag, percolate ion exchange method should be a fine default choice. But people have to pay careful consideration to good capacity and high selectivity for Ca while choosing ion exchangers.Salts of heteropoly acid and subsequent ion exchangers are likely to be promising exchange materials because of their specific selectivity for certain ions even in low concentrations, especially in the treatment of water system containing the same valence ions that are superior. For example, the high concentration Mn^{2+} (about 2,000 mg L^{-1}) will have much of an effect on the removal of Ca^{2+} in relatively low level (about 300 mg L^{-1}). With these considerations, five pyrophosphate heteropoly acid salts were synthesized as the starting precursors for novel Ca ion exchangers, and their performances including exchange capacities and dynamic exchange behaviors for calcium and manganese were tested. The selectivity for Ca^{2+} was also tested in the wastewater from electrolytic manganese industry. All these evaluations were compared with zirconium phosphate (ZrP) and molecular sieves such as 13X and 5A which have special selectivity to calcium.

2. Experimental

2.1. Reagents and instruments

Aqueous solutions of $K_4P_2O_7$, $ZrOCl_2$, $TiCl_4$, Na_2MoO_4, Na_2WO_4, Na_2SiO_3, H_3PO_4, HCl, NaOH, and HNO_3 were prepared by dissolving corresponding reagents of analytical grade in deionized water. 13X and 5A, obtained from commercial sources, which have special selectivity to calcium.

PHS-3C digital pH meter (Tianjin Shengbang Sci. Instrument Co), HY-5A-type cyclotron oscillator (Jintan Ronghua Instrument Co., Ltd., China), M6 Atomic Absorption Spectrometer (AAS) (Thermo Electron Co., England), FT-IR Spectrometer (TENSOR 27, Bruker), scanning electron microscope (SEM) (Leo, USA, 435 VP) and Automatic surface area and porosity analyzer (Micromeritics ASAP 2420 V2.05 Isixport, USA).

2.2. Preparation for ion exchangers

2.2.1. Synthesis of salts of BAPP-type heteropoly acids

Five kinds of salts of heteropoly acids were prepared at room temperature. First, 1.0 mol L^{-1} potassium pyrophosphate and 1.0 mol L^{-1} solution A (Na_2MoO_4, Na_2WO_4, or Na_2SiO_3) were mixed against a certain ratio under a constant stirring. The pH of the mixture was adjusted by addition of hydrochloric acid or sodium hydroxide to the set point. A certain amount of 0.1 mol L^{-1} solution B ($TiCl_4$, $ZrOCl_2$) was added drop wise into the mixture above with continuous and gentle stirring until white precipitate was no longer generated. Then a diluted HCl or NaOH solution was added into the solution slowly until the pH of the mother solution reached to requirements for the following aging. This mixture was allowed to stand for 24 h, then the precipitates were filtered, washed with deionized water to neutral, and dried at 40°C in a vacuumed oven. The dried precipitates were then cracked and converted to H^+ form with a HNO_3 solution of 0.1 mol L^{-1} [13]. BAPP exchangers were then obtained with the necessary separation, water rinsing to the neutral and desiccation.

2.2.2. Synthesis of ZrP

ZrP was synthesized by adding 2.5 mol L^{-1} phosphorous acid into a mixture of pyrophosphate zirconium and 1.0 mol L^{-1} hydrochloric acid gradually with continuous stirring until the mole ratio of PO_4^{3-} to Zr^{4+} got to 2:1. Then the precipitate obtained was allowed to stand with the mother liquor for 24 h, filtered off by vacuum, washed with deionized water, and dried at 60°C in an oven [14]. The ZrP was finally got by treating the precipitate with deionized water.

2.2.3. Conversion of 13X and 5A into H^+ form

The H^+ form adsorbent was obtained by adding 13X or 5A spherical particles into 1.0 mol L^{-1} nitric acid against a solid–liquid ratio of 1:3 and shaking thoroughly [15]. Several repetitions of convertion were conducted to ensure complete transformation of molecular sieves. 13X and 5A particles in H^+ form were finally obtained by washing particles with deionized water to the neutral and dried at 40°C at vacuum.

2.3. Determination of ion exchange capacities

2.3.1. The saturated ion-exchange capacity S_tIEC(X)

S_tIEC(X) was determined by static equilibrium through batch experiment. A 0.50 g exchanger (dry basis) in H^+ form was placed in a 100 mL Erlenmeyer flask. After an addition of a solution containing metal ion X, the Erlenmeyer flask was placed on an oscillator for 12 h at a vibration of 180 r min^{-1}. The concentration of X in supernatant was measured by AAS. The above operation was repeated until no further variation in the concentration of X was noted with the lapse of time, indicating the achievement of exchanging balance [16]. The ion-exchange capacity StIEC(X) was calculated as:

$$S_t\mathrm{IEC}(X) = \sum_{i=1}^{n} (C_{0,X} - C_{i,X}) \frac{V}{M \times m} \quad (1)$$

where $C_{0,X}$ is the initial content of metal ion X in solution, mg L^{-1}; $C_{i,X}$ is the final content of metal ion X in solution, mg L^{-1}; V is the initial volume of X solution taken for analysis, L; m is the initial dry mass of ion exchanger taken for analysis, g; n is the number of experiments and M is the atom weight of metal ion X, g mol^{-1}.

2.3.2. The apparent ion-exchange capacity (AIEC) and static absorption rate

A 50 mL metal ion X in solution was placed in a 100 mL Erlenmeyer flask. After measuring the initial pH of the solution, a 0.50 g (dry mass) amount of exchanger was added into the flask and stirred continuously. Then the pH was recorded until equilibrium was attained. The pH was plotted against time to observe absorption rate. The concentration of X metal ion in supernatant was measured by AAS. AIEC(X) was determined from the following equation:

$$\mathrm{AIEC}(X) = \frac{(C_{0,X} - C_{i,X})V}{m} \quad (2)$$

where $C_{0,X}$ is the initial concentration of metal ion X in solution, mg L^{-1}; $C_{i,X}$ is the final concentration of metal ion X in solution, mg L^{-1}; V is the initial volume of metal ion X taken for analysis, L; m is the initial dry mass of ion exchanger taken for analysis, g.

2.4. Column dynamic exchange

For dynamic study, the fixed-bed adsorption experiments were conducted using a laboratory-scale column at ambient temperature. About 7 g dried Zirconium tungstophosphate (ZWPP) was packed into a column with an inside diameter of 0.012 m and a bed height of 0.135 m. Deionized water was used to wash the exchanger several hours to remove bubbles in the column before the experiments. The feed Ca^{2+} solution with 300 mg L^{-1} was passed downstream through the column at a constant flowing rate of 0.5 mL min^{-1}. The outgoing solution was sampled periodically to measure Ca concentration in it. The breakthrough curve was plotted by C_t/C_0 against time t.

2.5. Selectivity studies

Distribution coefficients (K_d) [17] were determined using one-component solution and real manganiferous wastewater (Table 1), and the selectivities were characterized by selectivity factor $\alpha(\alpha = K_d(X_1)/K_d(X_2))$. The exchanger was placed into manganiferous wastewater with a dosage of 10 g L^{-1}. After being vibrated 12 h on the oscillator, the concentrations of metal ions in supernatant were measured by AAS, and the distribution coefficients $K_d(X)$ were determined from the following equation:

$$K_d(X) = \frac{C_{0,X} - C_{i,X}}{C_{i,X}} \times \frac{V}{m} \quad (3)$$

Table 1
Chemical composition of wastewater

Major ingredient	Ca^{2+}	Mn^{2+}	Mg^{2+}	SO_4^{2-}	F^-	HCO_3^-
Contents (mg L^{-1})	308.5	1,997.4	985.9	7,497.0	133.5	102.7

where $C_{0,X}$ is the initial amount of metal ion X in solution, mg L^{-1}; $C_{i,X}$ is the final amount of metal ion X in solution, mg L^{-1}; V is the initial volume of metal ion X taken for analysis, L; and m is the initial dry mass of ion exchanger taken for analysis, g.

2.6 Characterization

FT-IR was used to confirm the structures of the adsorbents. The dry exchangers were blended separately with KBr and pressed into pellets for analysis under a resolution of 2 cm^{-1} and a wave number range from 400 to 4,000 cm^{-1}.

Surface and pore morphology were observed by SEM at 40.0 kV. Simple particle size distribution was calculated by a software named Nano Measurer from SEM pictures.

Pore type and surface area were analyzed through BJH (Barrett Joiner Halenda) and BET (Brunauer Emmet Teller) models, respectively, using the automatic surface area and porosity analyzer.

3. Results and discussion

3.1. Characterization

The FT-IR spectra of the five heteropoly acid salts exchangers (Fig. 1) show the presence of extra water molecules besides hydroxyl groups and metal oxide groups in the materials. The strong and broad peak around 3,500 cm^{-1} and sharp peak around 1,600 cm^{-1} are assigned to the symmetric stretching vibration of interstitial water and bending vibration of free water, respectively [18]. The adsorption band at 1,340 cm^{-1}should be due to metal oxides insoluble in the structure and the broad band at 1,100–500 cm^{-1} exhibits the characteristic of metal-oxo stretching bands in the structure [19]. The broad band at 1,000 –1,100 cm^{-1} due to the bending vibration of P–O–P and the peak near 520 cm^{-1} is bending vibration of O–P–O. 600 and 400 cm^{-1} are the characteristic absorption peaks of Zr-O or Ti–O. The smaller peaks near 765 and 910 cm^{-1} should be assigned to vibration adsorption of W–O–W, Mo–O–Mo, or Si–O–Si [20]. All above could be ascribed to their Lacunary Keggin structure.

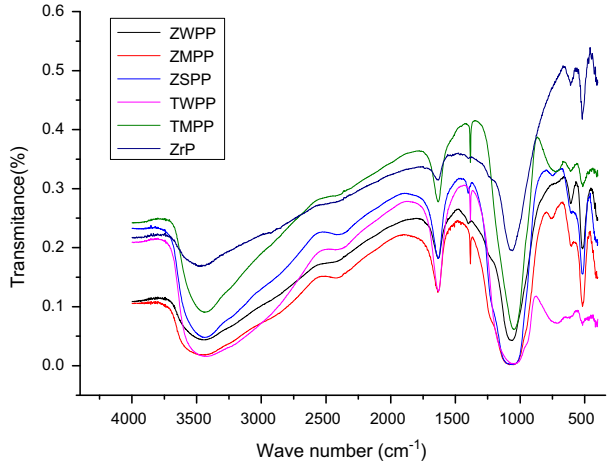

Fig. 1. FT-IR spectrum of ion exchangers.

SEM was used to observe the surface and pore morphology of the exchangers as shown in Fig. 2. The salts are all composed of particles of nanodimension and display special porous structures. Their surfaces are wrinkled and rucked up with the tolerable evenly distributed porosities, which are more conductive to adsorption of metal ions to adsorbents. Among them, ZWPP is more rugged and looser, its porous structure is more apparent. The particle sizes were also simulated and calculated. The results are listed in Table 2, and it can be found that the analogous particles have a size distribution between 300 and 600 nm.

The surface and porosity of ZWPP were analyzed on a Micromeritics analyzer. The results suggested that ZWPP may be in a list of mesoporous materials, as discussed in Section 3.6.

3.2. Saturated ion-exchange capacity

The ion-exchange capacity is one of the most important properties of an exchanger, as exchange capacity measurements provide a simple and direct way of characterizing an ion-exchanger sample. The ion-exchange capacities of five salts of heteropoly acid for Ca^{2+} and Mn^{2+} were tested and compared with ZrP and two zeolites. The data are listed in Table 3.

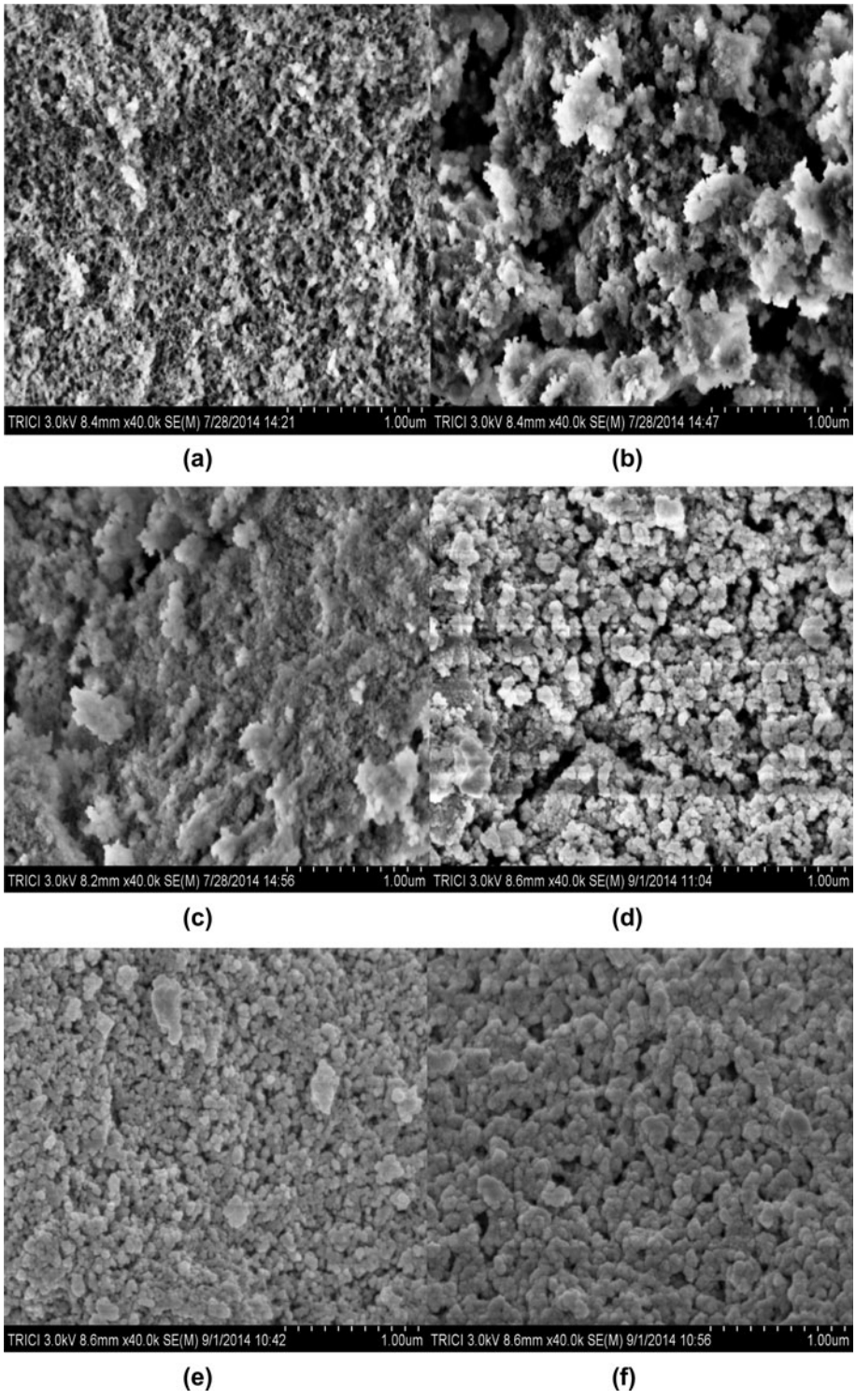

Fig. 2. SEM images: (a) ZWPP; (b) ZMPP; (c) ZSPP; (d)TWPP; (e) TMPP; and (f) ZrP.

The initial concentrations of Ca^{2+} and Mn^{2+} were modulated at 300 and 2,000 mg L^{-1}, respectively, simulating the wastewater from EMM industry. The results showed that the exchange abilities of these exchangers varied depending on their different chemical components and structures.

Table 2
Particle size distribution

Samples	Particle size range (nm)	Content (%)	Average particle size (nm)
ZWPP	300–600	95.06	350
ZMPP	200–400	92.61	340
ZSPP	300–500	88.95	340
ZrP	400–600	82.06	480
TWPP	300–600	94.02	390
TMPP	300–500	86.20	350

Table 3
S_tIEC of exchangers

Samples	IEC (Ca)[a] (mmol g^{-1})	IEC (Mn)[b] (mmol g^{-1})
ZWPP	0.6235	1.2055
ZMPP	0.2944	1.3708
ZSPP	0.6160	0.9851
ZrP	0.6709	0.5870
TWPP	0.2797	0.6806
TMPP	0.2802	0.5799
5A	0.8323	0.6054
13X	1.0841	0.6511

[a]C_0, Ca = 300 mg L^{-1}.
[b]C_0, Mn = 2,000 mg L^{-1}.

Adsorption performances of zirconium salts for Ca^{2+} adsorption are superior to titanium salts, although they all have some gaps with molecular sieves. It is imperative that Mn existence impose stiff competition on Ca exchange due to its chemical and charge properties, and much high concentration in potential applications in wastewater treatment for EMM industry. Therefore, the ion-exchange capacities of manganese were determined at the initial Mn concentration of 2,000 mg L^{-1} similar to real picture in slag leachate from EMM industry. Taking the above facts into account, ZWPP and ZSPP are much better than the others, as shown in Table 3.

3.3. Apparent ion-exchange capacity

The AIEC (Table 4) may likely reflect the effective exchange ability of an exchanger better while the S_tIEC is just nearly equal to the exchange capacity of the exchanger in theory. The AIEC(Ca) of zirconium salts is more than double of those for molecular sieves and ten folds of ones for titanium salts, although their AIECs(Mn) are also relatively higher, but considering the initial content of Mn^{2+} is nearly seven times of the level of Ca^{2+}, zirconium salts also appear to be promising ion exchangers. There are two kinds of exchange reactions: one is ion replacement on the surface of an exchanger, and the other is the ion diffusion within the inside of the exchanger. The AIEC(Ca)/S_tIEC(Ca) of zirconium salts are 37 and 40%, bigger than any others, and as about five times as molecular sieves. Among them, ZWPP, valued as 39.21%, is supreme, which proves that the exchange reactions mainly occurred inside the exchangers. It can be deduced that the exchange-adsorption rates of zirconium salts may be greater than others, thereby sooner equilibrium for it.

3.4. Static and column dynamic exchange analysis

The static absorption-rate [21] can be observed by pH titration curve. The faster and the greater the pH change, the higher the exchange-adsorption rate is, and consequently, the shorter time the equilibrium takes. The pH titration curves for Ca^{2+} are shown in Fig. 3(a). It can be observed that the obvious pH shifts downward for solutions with molecular sieves occurred around at 20 min and thereafter lasted for about 20 min. The variation was about 2.0 in pH. Then the pH values did not change significantly. These showed that the ion exchange mainly happened within the period of 20–40 min on the zeolites. By contrast, the pH of solutions with heteropoly acid salts changed immediately and sharply once the exchanger particles had been added into the solutions. The exchange for the salts above finished within only about 5–10 min [22] with a pH change of 3.0–4.5, and thereafter the curve went flat and remained that way smoothly. The pH curves for Mn^{2+} are shown in Fig. 3(b) and presented quite similar profiles to that in Fig. 3(a). In other words, exchange capacities and absorption rates for salts of heteropoly acids are significantly superior to the molecular sieves.

Moreover, it was observed that the solutions with the molecular sieves, especially for 13X, became cloudy and turbid after exchanging, and the particles of molecular sieves turned to be smaller than before

Table 4
AIEC of exchangers

Samples	AIEC(Ca)[a] (mmol g^{-1})	AIEC(Mn)[b] (mmol g^{-1})	AIEC (Ca)/IEC (Ca) (%)
ZWPP	0.2445	0.3616	39.21
ZMPP	0.1098	0.4727	37.28
ZSPP	0.2320	0.3538	37.66
ZrP	0.1372	0.1525	20.45
TWPP	0.0275	0.1386	9.81
TMPP	0.0125	0.1051	4.45
5A	0.0549	0.0098	6.59
13X	0.0873	0.0144	8.05

[a]C_0, Ca = 300 mg L^{-1}.
[b]C_0, Mn = 2,000 mg L^{-1}.

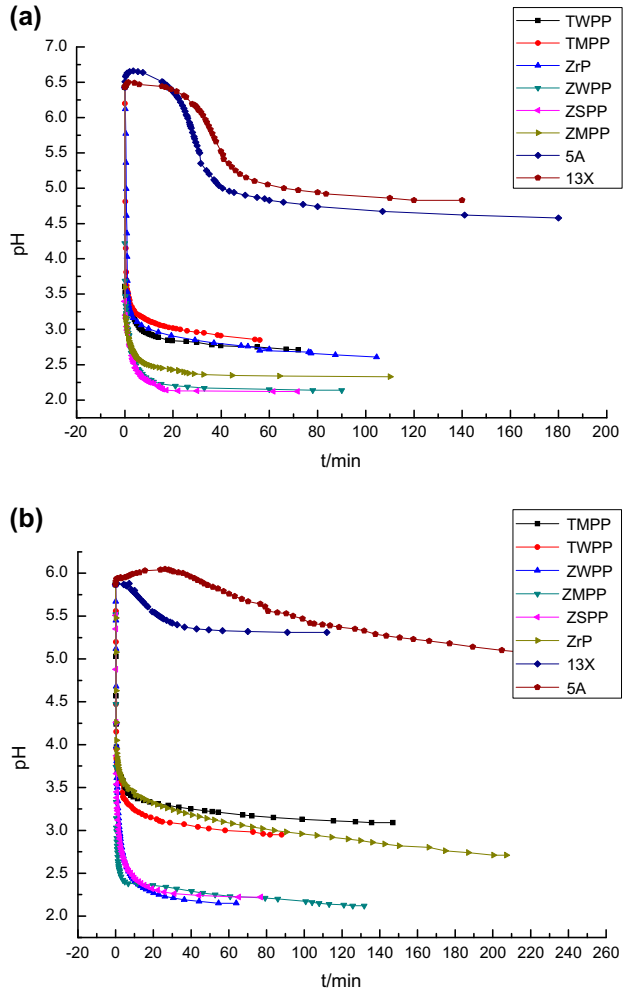

Fig. 3. pH-t curve: (a) for Ca^{2+} and (b) for Mn^{2+}.

and some were broken. That is to say, their physical structures were destroyed to some extent. The muddiness did not appear in the solutions with various salts including ZrP; little change in particle size was hinted, of course, it could not be judged explicitly without any further observation due to their unevenness in size derived from the nature of present preparation. We may do further observation when the crunch comes.

3.5. Adsorption selectivity

Selectivity for Ca^{2+} was characterized by distribution coefficients ($K_d(X)$) and selectivity factor ($\alpha = K_d(X_1)/K_d(X_2)$).

Distribution coefficients for the metal ions were determined in one-component solution (Table 5) and a real manganiferous wastewater (Table 6) in which the major cations were Mn^{2+}, Mg^{2+} and Ca^{2+} as shown in Table 1.

The higher distribution coefficient means better selectivity for the target ion. The results showed that the K_d(Ca) of zirconium salts are bigger than those for ZrP and molecular sieves. It indicated that the

Table 5
Distribution coefficients in one-component solution

Sample	K_d (Ca)[a]	K_d (Mn)[b]	K_d (Mg)[c]
ZWPP	91.2777	22.4290	11.8385
ZMPP	8.4128	18.1335	9.9795
ZSPP	26.4702	20.2935	13.2379
ZrP	19.1043	10.8893	12.2056
TWPP	19.8466	6.4736	5.2999
TMPP	42.1868	14.2596	5.6029
5A	26.7106	5.41850	2.7725
13X	17.1786	4.12330	2.1539

[a]C_0, Ca = 308.5 mg L^{-1}.
[b]C_0, Mn = 1,997.4 mg L^{-1}.
[c]C_0, Mg = 985.9 mg L^{-1}.

Table 6
Distribution coefficients and selectivity factors of exchangers in manganiferous waste water

Sample	K_d (Ca)[a]	K_d (Mn)[b]	K_d (Mg)[c]	K_d (Ca)/K_d (Mn)	K_d (Ca)/K_d (Mg)
ZWPP	16.7370	2.3091	4.1113	7.2484	4.0709
ZMPP	12.1257	2.5555	4.1489	4.7449	2.9226
ZSPP	12.7994	2.6412	6.9553	4.8460	1.8403
ZrP	3.2080	1.3144	9.6544	1.0589	0.3323
TWPP	4.8743	0.6506	2.8259	7.4924	1.7248
TMPP	2.7806	0.4165	4.1444	6.6767	0.6709
5A	4.4472	0.3750	0.5561	11.8604	7.9975
13X	3.1947	0.2002	0.5426	15.9618	5.8883

[a]C_0, Ca=308.5 mg L^{-1}.
[b]C_0, Mn = 1,997.4 mg L^{-1}.
[c]C_0, Mg = 985.9 mg L^{-1}.

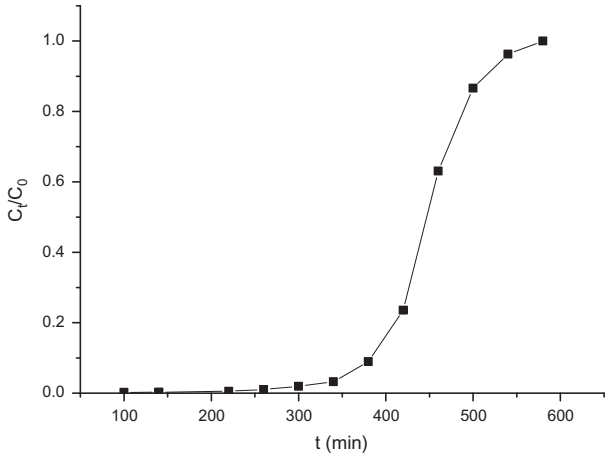

Fig. 4. Breakthrough curve of ZWPP with 300 mg L^{-1} calcium solution.

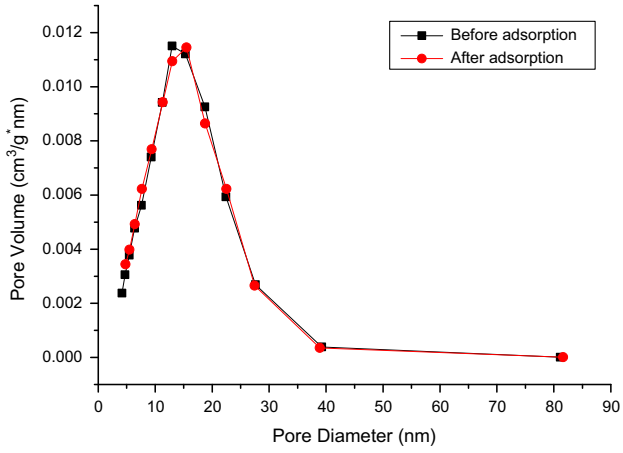

Fig. 6. ZWPP Dubinin–Astakhov plots for pore diameter before and after calcium absorption.

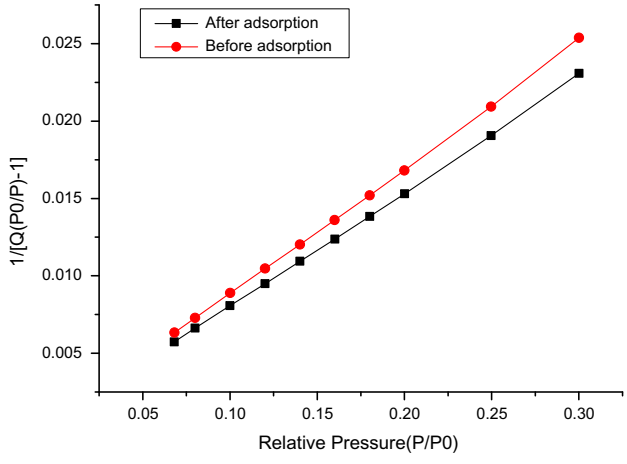

Fig. 5. BET surface area plots before and after calcium adsorption.

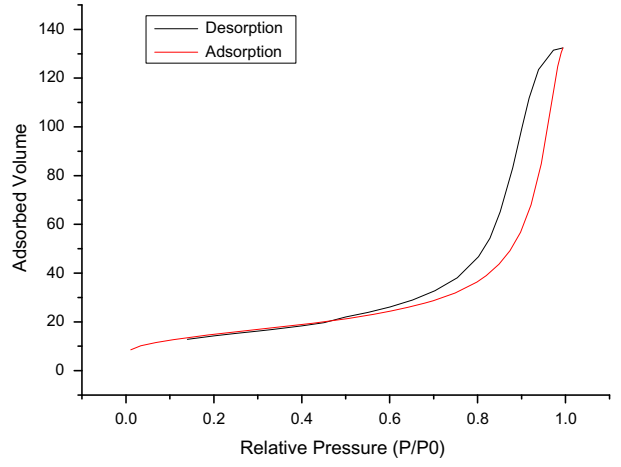

Fig. 7. ZWPP adsorption isotherm plots of adsorption and desorption.

zirconium salts have better selectivities to Ca, and it is understandable that K_d(Mn) and K_d(Mg) for the zirconium salts were quite big due to relatively large Mn and Mg quantities in the wastewater. This should be paid enough attention to in practical applications. In fact, the different exchangers made of different compositions of salts can be chosen for different treatment depending on enrichment factors for recovery or removal of metal.

When other ions coexist, the selectivity toward target ion X_1 will be affected by them and this effectiveness can be characterized by selectivity factor ($\alpha = K_d(X_1)/K_d(X_2)$). The higher the selectivity factor, the better the separation is. The salts of heteropoly acids have certain selectivities for Ca and still look worse than do the molecular sieves more or less (Table 6) due to the vial of materials themselves. It was concluded that the cations and anions of these pyrophosphate heteropoly salts affect selectivity for calcium in the complex system. All zirconium salts are more selective and rendered bigger coefficients than titanium salts. As the same cation was considered, selectivities of tungstopyrophosphate salts toward Ca are better than those for spiked samples with Mo and Si; and among them, ZWPP served the best selectivity which was very close to the ones of molecular sieves.

3.6. Breakthrough curve and BET analysis for ZWPP

In view of remarkable performances for Ca^{2+} exchange, ZWPP was further studied here through column exchange and adsorption–desorption process on an automatic analyzer.

The breakthrough curve can be used to describe the performances of packed bed and its shape is a substantial characteristic in determining the operational and dynamic behavior of an adsorption on fixed bed [23]. The breakthrough curve of ZWPP was expressed with the ratio of the outlet to the inlet concentration (C_t/C_0) vs. time t (min) in Fig. 4. The breakthrough and exhaustion points were set at 10 and 95% (C_t/C_0), respectively. The total mass of metal adsorbed q_{total} on the column was calculated as 63.92 mg and the equilibrium metal uptake capacity q_e was 9.13 mg g^{-1} under the given feed concentration and flow rate. The equilibrium capacity is almost consistent with static adsorption result (9.78 mg g^{-1}). It indicated that the ZWPP has good dynamic adsorption-performance and promising application.

The specific surface areas and pore diameter distribution of ZWPP were tested using the automatic surface area and porosity analyzer. The surface areas before and after calcium adsorption were 53.00 and 58.19 $m^2 g^{-1}$, respectively, which was estimated using multipoint BET equation in the P/P_0 range of 0.05–0.35 (Fig. 5). The data for pore distribution was placed in Fig. 4. It showed that the calcium ion exchanger is a kind of mesoporous material, for the pore size came out in the range of 13.58–16.76 nm (Fig. 6). Adsorption isotherm hysteresis loop (Fig. 7) is classified to be type H1 (both ends open tubular structure). This kind of isotherm usually reflects the micropore filling phenomena of adsorbents such as molecular sieves or activated carbon and reversible chemisorption process, similar to Langmuir isotherm.

4. Conclusion

Five salts of pyrophosphate heteropoly acids were synthesized and characterized using FT-IR, SEM, and so on. Their ion-exchange capacities, exchange behaviors, and selectivities for Ca^{2+} were tested and also compared with ZrP and two typical Ca-zeolites. All of them possessed specific capacities and selectivities for Ca^{2+}, even in complex industrial effluent. The results suggested that ZWPP was more remarkable. So, the dynamic capacities, special surface areas, and pore diameter of ZWPP were observed through column experiment and BET analysis. The data verified that ZWPP have good dynamic performances for Ca exchange with its mesoporosity and nanoparticles. Moreover, the stabilities, especially physical and mechanical stabilities of the salts, should be further studied and unambiguously characterized to develop ideal ion exchangers. Therefore, the salts of pyrophosphate heteropoly acids, especially ZWPP, can be used as promising precursor or materials for Ca removal from processing water and effluents in metallurgical industries.

References

[1] S. Dagnino, B. Picot, A. Escande, P. Balaguer, H. Fenet, Occurrence and removal of endocrine disrupters in wastewater treatment plants for small communities, Desalin. Water Treat. 4 (2009) 93–97.
[2] P.V.X. Hung, S.H. Cho, J.J. Woo, S.H. Moon, Behaviors of commercialized seawater reverse osmosis membranes under harsh organic fouling conditions, Desalin. Water Treat. 15 (2010) 48–53.
[3] Inamuddin, Yahya A. Ismail, Synthesis and characterization of electrically conducting poly-o-methoxyaniline Zr(IV) molybdate Cd(II) selective composite cation-exchanger, Desalination 250 (2010) 523–529.
[4] E.E. Özbaş, A. Öngen, C.E. Gökçe, Removal of astrazon red 6B from aqueous solution using waste tea and spent tea bag, Desalin. Water Treat. 51 (2013) 7523–7535.

[5] R. Yavari, S.J. Ahmadi, Y.D. Huang, A.D. Khanchi, G. Bagheri, J.M. He, Synthesis, characterization and analytical application of a new inorganic cation exchanger-titanium(IV) molybdophosphate, Talanta 77 (2009) 1179–1184.
[6] M.G. Ghannadi Marageh, S.W. Waqif Husain, A.R. Khanchi, S.J. Ahmady, Sorption studies of radionuclides on a new ion exchanger: Cerium (III) silicate, Appl. Radiat. Isot. 47 (1996) 501–505.
[7] J.L. Santos, I. Aparicio, A. Santos, F. Álvarez, M. López-Artíguez, D. Olano, S. García, E. Alonso, Presence of organic pollutants in sludge from anaerobic wastewater stabilization ponds, Desalin. Water Treat. 4 (2009) 116–121.
[8] P.G. Chithra, R. Raveendran, B. Beena, Parachlorophenol anchored tin antimonate-an inorgano-organic ion-exchanger selective towards heavy metals like Bi(III) and Cu(II), Desalination 232 (2008) 20–25.
[9] Y. Park, Y.C. Lee, W.S. Shin, S.J. Choi, Removal of cobalt, strontium and cesium from radioactive laundry wastewater by ammonium molybdophosphate–polyacrylonitrile (AMP–PAN), Chem. Eng. J. 162 (2010)685–695.
[10] V. Avramenko, S. Bratskaya, V. Zheleznov, I. Sheveleva, O. Voitenko, V. Sergienko, Colloid stable sorbents for cesium removal: Preparation and application of latex particles functionalized with transition metals ferrocyanides, J. Hazard. Mater. 186 (2011) 1343–1350.
[11] K. Lv, L.P. Xiong, Y.M. Luo, Ion exchange properties of cesium ion sieve based on zirconium molybdopyrophosphate, Colloids Surf., A 433 (2013) 37–46.
[12] M.M. Abd El-LatifM.F. Elkady, Kinetic study and thermodynamic behavior for removing cesium, cobalt and nickel ions from aqueous solution using nano-zirconium vanadate ion exchanger, Desalination 271 (2011) 41–54.
[13] H.Y. Zhang, S.L. Wang, R.S. Wang, C.S. Lin, X.Y. Zhang, X.R. Wang, New ecomaterialzireonyl molybopyrophosphate for cesium removal from HLLW, Acta Physico-Chim. Sin. 16 (2000) 952–955.
[14] S.A. Shady, Selectivity of cesium from fission radionuclides using resorcinol-formaldehyde and zirconyl-molybdopyrophosphate as ion-exchangers, J. Hazard. Mater. 167 (2009) 947–952.
[15] Z.M. Siddiqi, D. Pathania, Titanium(IV) tungstosilicate and titanium(IV) tungstophosphate: two new inorganic ion exchangers, J. Chromatogr. A. 987 (2003) 147–158.
[16] H.X. Zhang, Synthesis and study of a new inorganic ion-exchanger: Titanium(IV) tungstopyrophosphate, Ind. Water Treat. 21 (2001) 26–28 (in Chinese).
[17] M. Qureshi, R. Kumar, H.S. Rathore, Studies on chromium(III) hydroxide, arsenate, antimonate, molybdate and tungstate, Talanta 19 (1972) 1377–1386.
[18] H.Y. Zhang, R.S. Wang, C. Sh Lin, X.Y. Zhang, Preparation, structure and application of a new ecomaterials cesium ion-sieve, Prog. Nat. Sci. 12 (2002) 91–95.
[19] F.M. Zonoz, S.J. Ahmadi, A.S. Nosrati, M.G. Maragheh, Preparation and characterization of zirconium (IV) molybdo tungsto vanado silicate as a novel inorganic ion exchanger in sorption of radionuclides, J. Hazard. Mater. 169 (2009) 808–812.
[20] L.L. Zhao, H.Y. Zhang, X.R. Wang, Developing of cesium ion-sieve, Yunnan Environ. Sci. S1 (2000) 35–39 (in Chinese).
[21] I.P. Saraswat, S.K. Srivastava, A.K. Sharma, A study on the kinetics and mechanism of exchange of rubidium and cesium in chromium ferrocyanide gel using radioactive tracers, J. Inorg. Nucl. Chem. 43 (1981) 1653–1657.
[22] S.D.W. Comber, M.J. Gardner, A.M. Gunn, C. Whalley, Kinetics of trace metal sorption to estuarine suspended particulate matter, Chemosphere 33 (1996) 1027–1040.
[23] A.A. Ahmad, B.H. Hameed, Fixed-bed adsorption of reactive azo dye onto granular activated carbon prepared from waste, J. Hazard. Mater. 175 (2010) 298–303.